Nonlinear Analysis: Modelling and Control, Vol. 31, No. 1, 68–92
https://doi.org/10.15388/namc.2026.31.44130

Vilnius University Press

An analytical study of the time-fractional extended shallow-water wave equation in $(3+1)$-dimension with two different derivatives and their comparison

Esra Ünal Yılmaz[a], **Yeşim Sağlam Özkan**[b]

[a]Department of Mathematics, Bolu Abant Izzet Baysal University, Bolu, Turkey
esraunal@ibu.edu.tr

[b]Department of Mathematics, Bursa Uludag University, Bursa, Turkey
ysaglam@uludag.edu.tr

Received: January 30, 2025 / **Revised:** August 22, 2025 / **Published online:** January 1, 2026

Abstract. In ocean physics, an essential mathematical framework for examining the dynamic behavior of waves is the $(3+1)$-dimensional generalized shallow-water wave equation. This approach is driven by the growing need to incorporate nonlinear and anomalous behaviors in shallow-water wave propagation into more realistic mathematical models. This motivation is a key consideration for improving coastal hazard prediction, mitigating tsunami impacts, optimizing renewable energy extraction, and deepening our understanding of complex coastal processes. In this paper, exact solutions of the fractional generalized shallow-water wave equation are constructed using two alternative methods: the extended modified auxiliary equation mapping method and the F-expansion approach. The extended modified auxiliary equation mapping method yielded nineteen exact solutions across two main sets, while the F-expansion method produced solutions for seventeen different cases. To visualize these, 2D and 3D graphical representations have been generated for several solutions using fractional parameter values $\alpha \in (0,1]$, including sample values such as 0.2, 0.5, 0.7, and 0.78, to illustrate how the order of the derivative affects the soliton profile. The results show that decreasing α leads to broader and smoother soliton structures. Finally, the modulation instability of the governing model is also investigated, confirming that the established results are stable.

Keywords: the extended modified auxiliary equation mapping method, the F-expansion method, M-truncated derivative, β-derivative, shallow-water wave equation, modulation instability.

1 Introduction

Nonlinear evolution equations (NLEEs) occupy an important place in mathematical physics and differential equations. They model the evolution of systems over time and describe nonlinear behaviors. Fields such as elasticity theory, wave motion, fluid dynamics, thermodynamics, biological systems, and certain chemical processes require their solutions. The development of nonlinear equations accelerated with the discovery of soliton theory,

and in the 1960s, the Korteweg–de Vries (KdV) equation became a key example. In recent years, shallow-water wave equations have received considerable attention, modeling situations where water depth is much smaller than the wavelength of surface disturbances. These equations are often fully integrable and admit solitary and cnoidal wave solutions.

In order to investigate a variety of exact and explicit solutions, numerous schemes have been established. These include, for example, the $(G'/G, 1/G)$-expansion method [20], the Bernoulli subequation function method [3], the Jacobi elliptic function expansion method [1], the unified auxiliary equation method [2], the improved $\tan(\phi/2)$-expansion method [19], and so on. Each of these analytical methods has demonstrated efficacy in obtaining precise solutions for nonlinear evolution equations with diverse structural attributes. Several studies in the literature have demonstrated the applicability, reliability, and efficiency of various methods in capturing the intricate behaviors of nonlinear physical systems [18, 25, 27].

Fractional-order derivatives are a mathematical generalization of the derivative that allows for derivatives of functions of any real or complex order. This method often reveals finer details of a function. Although the first theories of fractional derivatives were developed in the 19th century, there has been significant progress in recent years. These derivatives are used to model complex behavior in various systems. Some examples are the Riemann–Liouville [21], Caputo derivative [5], Gerasimov–Caputo [11], and Atangana–Baleanu derivatives [6]. These operators offer a flexible mathematical framework for studying memory and genetic characteristics in complex systems.

Nonlinear $(2+1)$- and $(3+1)$-dimensional equations explain real aspects of science, technology, oceanography, atmosphere, and engineering. Physical space-time models are realistically represented by $(3+1)$-dimensional systems, which motivates the study of higher-dimensional, especially integrable, models. Solving these equations accurately plays a major role in comprehending different aspects of nonlinear scientific processes, both qualitative and quantitative. The $(2+1)$-dimensional shallow-water wave equations [10, 29] are given as

$$u_{yt} + u_{xxxy} - 3u_{xx}u_y - 3u_x u_{xy} = 0, \tag{1}$$

$$u_{xt} + u_{xxxy} - 2u_{xx}u_y - 4u_x u_{xy} = 0, \tag{2}$$

where $u = u(x, y, t)$. In the case of $x = y$, both equations (1) and (2) are reduced to the potential KdV equation. In [10, 28, 29], the following $(3+1)$-dimensional shallow-water wave equations are considered:

$$u_{yzt} + u_{xxxyz} - 6u_x u_{xyz} - 6u_{xz}u_{xy} = 0, \tag{3}$$

$$u_{xzt} + u_{xxxyz} - 2(u_{xx}u_{yz} + u_y u_{xxz}) - 4(u_x u_{xzy} + u_{xz}u_{xy}) = 0, \tag{4}$$

where $u = u(x, y, z, t)$. For $x = y = z$, Eqs. (3) and (4) reduce to the potential KdV equation. The extended shallow-water wave equation in $(3+1)$ dimension reads as [7, 30]

$$w_{xzt} + w_{xxxyz} - 2(w_{xx}w_{yz} + w_y w_{xxz}) - 4(w_x w_{xyz} + w_{xz}w_{xy}) + \beta w_{xyz} = 0, \tag{5}$$

where $w = w(x, y, z, t)$, and β is constant. The extended shallow-water wave equation generalizes the classical form and is often used to model wave propagation with more general nonlinearities than the KdV equation. In many real-world systems, memory and hereditary effects described by fractional derivatives are significant, especially in porous layers, viscoelastic fluids, and plasmas [17]. Employing fractional derivatives (e.g., β and M-truncated types) provides a flexible framework to capture these effects with variations in amplitude, steepness, and dispersion reflecting realistic wave behavior in complex media. Such models are relevant not only for coastal and ocean engineering but also for nonlinear optics, where similar equations describe pulse propagation in optical fibers and photonic lattices [17]. In this context, treating Eq. (5) as a time-fractional equation aids in understanding its dynamics. In this work, the following fractional version of Eq. (5) will be discussed:

$$\begin{aligned} &D_t^{\alpha} w_{xz} + w_{xxxyz} - 2(w_{xx}w_{yz} + w_y w_{xxz}) \\ &\quad - 4(w_x w_{xyz} + w_{xz}w_{xy}) + \beta w_{xyz} = 0, \end{aligned} \tag{6}$$

where spatial variations are denoted by x, y, and z, the temporal evolution of the wave by t, while β is constant, and α is an order of the fractional derivative. The fractional derivative (D_t^{α}), which satisfies the requirements for both integer- and fractional-order derivatives, is taken into consideration here. In ocean physics, a central motivation for this study is the need to develop more realistic mathematical models that capture the nonlinear and anomalous behaviors observed in shallow-water wave dynamics. The $(3 + 1)$-dimensional generalized shallow-water wave equation provides a powerful framework for analyzing such complex wave phenomena. By advancing our understanding of these dynamics, this approach contributes to critical applications such as enhancing coastal hazard prediction, mitigating the effects of tsunamis, optimizing the design of renewable energy systems, and uncovering the intricacies of nearshore and coastal processes.

While the current study focuses on traveling and solitary wave solutions of the $(3+1)$-dimensional fractional derivative model, other nonlinear wave structures, such as lump and rogue waves, have attracted attention due to their unique physical relevance. Lump solutions are localized in all spatial directions and describe multidimensional wave patterns [16], while rogue waves are transient, large-amplitude events often modeled through rational solutions. Several recent works have explored these structures in fractional and higher-dimensional nonlinear evolution equations [8, 9, 15]. Although our analysis does not include them, future studies could extend our methodologies to investigate lump or rogue wave dynamics within the fractional framework.

Traveling wave solutions of nonlinear differential equations can be obtained using various methods, including the extended modified auxiliary equation mapping method. This approach enhances solution finding by allowing diverse algorithms and more general auxiliary equations to be incorporated into the analytical process. It systematically produces solutions for solitons, kinks, pulse-type and periodic waves, making it a versatile tool for modeling nonlinear phenomena [24].

Additionally, the F-expansion method effectively obtains a wide variety of accurate traveling wave solutions for NLEEs. Key advantages of the F-expansion method

include structural simplicity, ease of application to many types of nonlinear equations, and the ability to produce a wide family of solutions, including symmetric structures. The method's success with soliton solutions makes it practically applicable in disciplines such as mathematical physics, engineering, and biology. The method offers a strong, flexible alternative in terms of solution diversity. Furthermore, these methods are well suited for symbolic computations using algebraic software tools such as Maple and Mathematica. Their algorithmic structure reduces the likelihood of human error, especially when dealing with complex expressions.

It is imperative to note that the reduced computational time and efficiency of our techniques are fundamental factors in elucidating their simplicity, reliability, accuracy, and ease of use. Although the methods used in this study yield a wide range of exact traveling wave solutions, they are limited by their dependency on specific ansatz forms and may not capture all possible solution behaviors, especially in more complex or multiscale settings.

The paper is divided into distinct sections. In Section 2, we provide some basic definitions of fractional calculus. In Section 3, we describe the governing system from a mathematical perspective. In Section 4, we give the brief descriptions of the F-expansion and the extended modified auxiliary equation mapping methods. In Section 5, we present the applications of the aforementioned techniques to get soliton solutions. In Section 6, we describe some gained results by 2D, 3D, and contour plots, and we looked at how to interpret the graphs and make the required comparisons. In Section 7, we determine stability analysis for the stationary solutions of (5). In the last section, we present the conclusion.

2 Basic definitions of calculus

In this section, the definitions of the M-truncated fractional derivative and the β-fractional derivative, along with some of their properties, are presented.

2.1 M-truncated fractional operator

Definition 1. Suppose that

$$f(t) : [0, \infty) \to \mathbb{R}$$

and $0 < \alpha < 1$, then M-truncated derivative of f of order α is defined by [13, 26]

$$D_M^{\alpha,\theta} f(t) = \lim_{\tau \to 0} \frac{f(t + {}_iE_\theta(\tau t^{1-\alpha})) - f(t)}{\tau}, \quad \theta > 0,$$

for $t > 0$. Here ${}_iE_\theta(z) = \sum_{j=0}^{i} z^j/\Gamma(\theta j + 1)$, $\theta > 0$, and $z \in \mathbb{C}$ is truncated Mittag-Leffler function of one parameter [26].

Theorem 1. *If f is a α-order differentiable function with α in $(0, 1]$ and $\theta > 0$ at $t_0 > 0$, then f is continuous at t_0.*

Theorem 2. *If $\alpha \in (0, 1]$, $\theta > 0$, $k, l \in \mathbb{R}$, and f and h are α-differentiable at $t > 0$, then*:

(i) $D_M^{\alpha,\theta}(kf(t)+lh(t)) = kD_M^{\alpha,\theta}(f(t)) + lD_M^{\alpha,\theta}(h(t))$;
(ii) $D_M^{\alpha,\theta}(f(t),h(t)) = f(t)D_M^{\alpha,\theta}(h(t)) + h(t)D_M^{\alpha,\theta}(f(t))$;
(iii) $D_M^{\alpha,\theta}(f(t)/h(t)) = (h(t)D_M^{\alpha,\theta}(f(t)) - f(t)D_M^{\alpha,\theta}(h(t)))/(h(t))^2$;
(iv) $D_M^{\alpha,\theta}(\tau) = 0$, *where* τ *is a constant*;
(v) *If* $f(t)$ *is differentiable, then* $D_M^{\alpha,\theta}(f(t)) = (t^{1-\alpha}/\Gamma(\theta+1))\,\mathrm{d}f(t)/\mathrm{d}t$.

2.2 β-fractional operator

Definition 2. The β-derivative [4, 22] of a function $f(\chi)$ of fractional order α is defined as

$$ {}_0^A D_\psi^\alpha\big(f(\chi)\big) = \lim_{\epsilon\to 0} \frac{f(\psi + \epsilon(\psi + \frac{1}{\Gamma(\alpha)})) - f(\chi)}{\epsilon}. $$

In addition, the following are some of this operator's known properties.

Theorem 3. *If* $0 < \alpha \leqslant 1$, $m, n \in \mathbb{R}$, *and* f *and* h *are the functions of order* α *at* $\chi > 0$ *given point, then*:

(i) ${}_0^A D_\chi^\alpha(mf(\chi) + nh(\chi)) = m{}_0^A D_\chi^\alpha(f(\chi)) + n{}_0^A D_\chi^\alpha(h(\chi))$;
(ii) ${}_0^A D_\chi^\alpha(\tau) = 0$, *where* τ *is constant*;
(iii) ${}_0^A D_\chi^\alpha(h(\chi) * f(\chi)) = h(\chi){}_0^A D_\chi^\alpha(f(\chi)) + f(\chi){}_0^A D_\chi^\alpha(h(\chi))$;
(iv) ${}_0^A D_\chi^\alpha(g(\phi)/h(\chi)) = \phi \mathrm{d}g(\phi)/\mathrm{d}\phi$;
(v) ${}_0^A D_\chi^\alpha(f(\chi)/h(\chi)) = (h(\chi){}_0^A D_\chi^\alpha(f(\chi)) - f(\chi){}_0^A D_\chi^\alpha(h(\chi)))/h^2(\chi)$.

Taking $\epsilon = (\chi + 1/\Gamma(\alpha))^{1-\alpha}c$, $\epsilon \to 0$ *as* $c \to 0$, *then we have*

$$ {}_0^A D_\chi^\alpha\big(f(\chi)\big) = \left(\chi + \frac{1}{\Gamma(\alpha)}\right)^{1-\alpha} \frac{\mathrm{d}f(\chi)}{\mathrm{d}\chi}, \qquad \zeta = \frac{\lambda}{\alpha}\left(\chi + \frac{1}{\Gamma(\alpha)}\right)^{\alpha}, $$

where the constant is denoted by λ.

3 Fractional governing equation

In this section, the time-fractional extended shallow-water wave equation (6), which will be discussed, will be reduced to an ordinary differential equation (ODE) using the definitions and properties of the introduced fractional derivative operators. For this purpose, two different traveling wave transformations will be employed.

(i) The following is the expression of the considered equation using the M-truncated fractional operator:

$$ \begin{aligned} &D_{M,t}^{\alpha,\gamma} w_{xz} + w_{xxxyz} - 2(w_{xx}w_{yz} + w_y w_{xxz}) \\ &\quad - 4(w_x w_{xyz} + w_{xz}w_{xy}) + \beta w_{xyz} = 0. \end{aligned} \tag{7} $$

(ii) For the β-derivative, we have

$$\begin{aligned} &{}_0^A D_t^\alpha w_{xz} + w_{xxxyz} - 2(w_{xx}w_{yz} + w_y w_{xxz}) \\ &\quad - 4(w_x w_{xyz} + w_{xz}w_{xy}) + \beta w_{xyz} = 0. \end{aligned} \tag{8}$$

Assume the following wave transformation in Eqs. (7) and (8):

$$w(x, y, z, t) = u(\xi).$$

$w(x, y, z, t)$ is the wave form of the solitons in this case. The variable representing the wave, designated as ξ, is defined as follows:

(i) For M-truncated fractional derivative,

$$\xi = kx + ly + nz - \delta \frac{\Gamma(1+\gamma)}{\alpha} t^\alpha. \tag{9}$$

(ii) For β fractional derivative,

$$\xi = kx + ly + nz - \frac{\delta(t + \frac{1}{\Gamma(\alpha)})^\alpha}{\alpha}. \tag{10}$$

Substituting Eqs. (9) and (10) in Eqs. (7) and (8) results in the subsequent equation

$$lk^2 u''' - 3lk(u')^2 + (-\delta + \beta l)u' = 0. \tag{11}$$

If $u' = v$, then $u'' = v'$ and $u''' = v''$, and (11) turns to be

$$lk^2 v'' - 3lkv^2 + (-\delta + \beta l)v = 0, \tag{12}$$

where $(\cdot)' = \mathrm{d}/\mathrm{d}\xi(\cdot)$.

4 Methodologies

The following section outlines the principal components of two widely-appreciated and efficacious methodologies for resolving the aforementioned equation. To this end, we take into account the following partial differential equation (PDE)

$$\Omega(\nu, \nu_t, \nu_x, \nu_{tt}, \nu_{tt}, \dots) = 0, \tag{13}$$

where Ω and its corresponding derivatives form a component of the dependent function $\nu = \nu(x, t)$. The travelling wave transformation is given by the following equation:

$$\nu = \nu(\xi), \quad \xi = k(x - ct),$$

where k and c are constants. Substituting the aforementioned expression into the Eq. (13), we obtain an ODE

$$\Lambda(\nu, \nu', \nu'', \dots) = 0, \tag{14}$$

where $(\cdot)'$ indicates the derivatives with respect to the independent variable ξ. The following algorithm outlines the general procedure for obtaining exact solutions of nonlinear evolution-type PDEs using analytical techniques.

Algorithm 1. Exact solution algorithm for nonlinear evolution equations.

1: **Identify the target PDE:** Begin with the nonlinear evolution equation to be solved.
2: **Apply a traveling wave transformation:** Introduce a new variable to reduce the PDE to an ODE.
3: **Reduce the PDE to an ODE:** Substitute the wave variable and convert the PDE into an ODE for $u(x,t) = U(\xi)$.
4: **Propose a suitable ansatz:** Depending on the chosen method, propose an appropriate functional form.
5: **Substitute the ansatz into the ODE:** Compute all necessary derivatives of the ansatz and substitute them into the ODE.
6: **Collect terms and construct an algebraic system:** Collect coefficients of functionally independent terms and equate each to zero to form a system of algebraic equations.
7: **Solve the algebraic system:** Solve the system to determine the unknown parameters using symbolic computation software (e.g., Maple, Mathematica).
8: **Construct the exact solution:** Substitute the obtained constants back into the ansatz to get the final solution in the form $u(x,t) = U(\xi)$.
9: **Analyze and classify the solution:** Interpret the solution in terms of physical or mathematical characteristics.

4.1 The extended modified auxiliary equation mapping method

The main steps of the extended modified auxiliary equation mapping method used in our paper can be considered as an improvement of that obtained in [23], which are described as follows:

Step 1. We assume that Eq. (14) has the solution of the form

$$\nu(\xi) = \sum_{j=0}^{m} a_j \mathcal{F}^j(\xi) + \sum_{j=-1}^{-m} b_{-j} \mathcal{F}^j(\xi) + \sum_{j=2}^{m} c_j \mathcal{F}^{j-2}(\xi)\mathcal{F}'(\xi) + \sum_{j=1}^{m} d_j \left(\frac{\mathcal{F}'(\xi)}{\mathcal{F}(\xi)}\right)^j, \quad (15)$$

where $F(\xi)$ satisfies the ODE

$$\mathcal{F}'^2 = \left(\frac{\mathrm{d}F}{\mathrm{d}\xi}\right)^2 = \mu_1 \mathcal{F}^2(\xi) + \mu_2 \mathcal{F}^3(\xi) + \mu_3 \mathcal{F}^4(\xi), \quad (16)$$

where a_j, b_j, c_j, d_j and μ_1, μ_2, μ_3 are the coefficients to be determined later. m is a positive integer.

Step 2. The integer m is determined by balancing the highest-order derivative term with the highest-order nonlinear term in the reduced ODE.

Step 3. After plugging Eq. (15) with Eq. (16) into ODE and equating coefficients of various powers of $\mathcal{F}^j(\mathcal{F}')^k$ ($k = 0, 1$; $j = 0, 1, 2, \ldots, m$), the system of algebraic equations is obtained.

Step 4. Subsequently, the utilization of a mathematical solver such as Maple, Mathematica, or Matlab will facilitate the identification of additional values for the constants, namely a_j, b_j, c_j, d_j.

Step 5. By putting all constant value into Eq. (15), all of the required solutions of the equation under consideration are obtained.

4.2 The F-expansion method

The main steps of the F-expansion method used in our paper can be considered as an improvement of that obtained in [12], which are described as follows:

Step 1. Let Eq. (14) have the solution of the form

$$\nu(\xi) = \sum_{i=0}^{s} a_i F^i(\xi), \tag{17}$$

where a_i are constants, and s is a positive integer that can be calculated by balancing principle. The auxiliary equation that follows is satisfied by $F(\zeta)$:

$$F'(\xi) = \sqrt{PF^4(\xi) + QF^2(\xi) + R}, \tag{18}$$

where the constants P, Q, and R are determined later. The following equations are available for Eq. (18):

$$F'' = 2PF^3 + QF, \quad F''' = (6PF^2 + Q)F', \ldots, \tag{19}$$

which will be used later on.

Step 2. Using computer programming, an algebraic system of equations can be derived by substituting (17) into (14), together with (18) (and (19)), then collecting coefficients of like terms of the form $F^i(F')^j$, where $j = 0, 1, \ldots$, $i = 0, 1, 2, \ldots$.

Step 3. Each of these coefficients is set equal to zero, resulting in a system of equations. By solving this system, the coefficients a_i for $i = 0, 1, \ldots, s$ are determined.

Step 4. Substituting these coefficients back into (17) then yields the exponential and periodic solutions. (18) holds with

$$F(\xi, m) = \operatorname{sn}(\xi, m), \quad P = 1, \quad Q = -1 - m^2, \quad R = 1, \tag{20_1}$$

$$F(\xi, m) = \operatorname{cn}(\xi, m), \quad P = -m^2, \quad Q = 2m^2 - 1, \quad R = -m^2 + 1, \tag{20_2}$$

$$F(\xi, m) = \operatorname{ns}(\xi, m), \quad P = 1, \quad Q = -m^2 - 1, \quad R = m^2, \tag{20_3}$$

$$F(\xi, m) = \operatorname{cs}(\xi, m), \quad P = 1, \quad Q = 2 - m^2, \quad R = 1 - m^2, \tag{20_4}$$

$$F(\xi, m) = \operatorname{ns}(\xi, m) \pm \operatorname{cs}(\xi, m), \quad P = \frac{1}{4}, \quad Q = \frac{1}{2} - m^2, \quad R = \frac{1}{4}, \tag{20_5}$$

$$F(\xi, m) = \frac{\operatorname{sn}(\xi, m)}{1 \pm \operatorname{cn}(\xi, m)}, \quad P = \frac{1}{4}, \quad Q = \frac{1}{2} - m^2, \quad R = \frac{1}{4}, \tag{20_6}$$

$$F(\xi, m) = \frac{m(\operatorname{sn}(\xi, m))^2 - 1}{B(m(\operatorname{sn}(\xi, m))^2 + 1)}, \quad P = -(m^2 + 2m + 1)B^2,$$
$$Q = 2m^2 + 2, \quad R = \frac{2m - m^2 - 1}{B^2}, \tag{20_7}$$

$$F(\xi, m) = \operatorname{dc}(\xi, m), \quad P = 1, \quad Q = -1 - m^2, \quad R = m^2, \tag{20_8}$$

$$F(\xi, m) = \operatorname{sc}(\xi, m), \quad P = -m^2 + 1, \quad Q = 2 - m^2, \quad R = 1, \tag{20_9}$$

$$F(\xi,m)=nc(\xi,m)\pm \mathrm{sc}(\xi,m),$$
$$P=\frac{1-m^2}{4},\quad Q=\frac{m^2+1}{2},\quad R=\frac{1-m^2}{4}, \tag{20$_{10}$}$$
$$F(\xi,m)=\frac{\mathrm{cn}(\xi,m)}{1\pm \mathrm{sn}(\xi,m)},$$
$$P=\frac{1-m^2}{4},\quad Q=\frac{m^2+1}{2},\quad R=\frac{1-m^2}{4}, \tag{20$_{11}$}$$
$$F(\xi,m)=\frac{\sqrt{\frac{C^2m^2+B^2-C^2}{C^2m^2+B^2}}+\mathrm{cn}(\xi,m)}{B\,\mathrm{sn}(\xi,m)+C\,\mathrm{dn}(\xi,m)},$$
$$P=\frac{C^2m^2+B^2}{4},\quad Q=\frac{1}{2}-m^2,\quad R=\frac{1}{4C^2m^2+4B^2}, \tag{20$_{12}$}$$
$$F(\xi,m)=\frac{\sqrt{\frac{-C^2m^2+B^2+C^2}{C^2+B^2}}+\mathrm{dn}(\xi,m)}{B\,\mathrm{sn}(\xi,m)+C\,\mathrm{cn}(\xi,m)},$$
$$P=\frac{C^2+B^2}{4},\quad Q=\frac{1}{2}m^2-1,\quad R=\frac{m^4}{4C^2+4B^2}. \tag{20$_{13}$}$$

5 Method applications

The extended modified auxiliary equation mapping approach and the F-expansion method will be used to analyze the solutions of Eq. (11) (and (12)) in this section.

5.1 The extended modified auxiliary equation mapping method

The extended modified auxiliary equation mapping method will be used in this section to derive and investigate the traveling wave solutions for the targeted model. After balancing u'' with $(u')^2$, we find that $m=1$ in Eq. (11). Substituting $m=1$ into Eq. (15) yields the following result:

$$u(\xi)=a_0+a_1F(\xi)+\frac{b_1}{F(\xi)}+d_1\frac{\frac{\mathrm{d}}{\mathrm{d}\xi}F(\xi)}{F(\xi)}.$$

It can be concluded from the steps outlined in Section 4.1 that the following results are obtained:

- Set 1: $\delta=l(k^2{\mu_2}^2+4\beta\mu_3)/(4\mu_3)$, $a_0=a_0$, $a_1=0$, $b_1=0$, $d_1=2k$, $\mu_1=\mu_2^2/(4\mu_3)$.

Therefore, we have the following solutions for Set 1:

$$w_1(x,y,z,t)=\frac{(4k\Upsilon+3a_0)\cosh(\Upsilon\xi)-\sinh(\Upsilon\xi)(4k\Upsilon-a_0)}{\sinh(\Upsilon\xi)+3\cosh(\Upsilon\xi)}, \tag{21}$$

where $\Upsilon=\sqrt{\mu_2^2/\mu_3}/4$, $\mu_3>0$, ξ is given in Eqs. (9) and (10);

$$w_2(x,y,z,t)=\frac{(-4k\Upsilon+a_0)\cosh(\Upsilon\xi)+\sinh(\Upsilon\xi)(4k\Upsilon+3a_0)}{\cosh(\Upsilon\xi)+3\sinh(\Upsilon\xi)}, \tag{22}$$

where $\Upsilon=\sqrt{\mu_2^2/\mu_3}/4$, $\mu_3>0$, ξ is given in Eqs. (9) and (10);

$$w_3(x,y,z,t)=-\frac{(8k\Upsilon-2a_0)(\cosh^2(\Upsilon\xi))+2\sinh(\Upsilon\xi)(4k\Upsilon-a_0)\cosh(\Upsilon\xi)-4k\Upsilon}{2\cosh(\Upsilon\xi)(\sinh(\Upsilon\xi)+\cosh(\Upsilon\xi))},$$

where $\Upsilon=\sqrt{\mu_2^2/\mu_3}/4$, $\mu_3>0$, ξ is given in Eqs. (9) and (10);

$$\begin{aligned}w_4(x,y,z,t)=-\big((8k\Upsilon-2a_0)\big(\cosh^2(\Upsilon\xi)\big)+2a_0-4k\Upsilon\\+2\sinh(\Upsilon\xi)(4k\Upsilon-a_0)\cosh(\Upsilon\xi)\big)\\\times\big(2\sinh(\Upsilon\xi)\big(\sinh(\Upsilon\xi)+\cosh(\Upsilon\xi)\big)\big)^{-1},\end{aligned}$$

where $\Upsilon=\sqrt{\mu_2^2/\mu_3}/4$, $\mu_3>0$, ξ is given in Eqs. (9) and (10);

$$\begin{aligned}w_5(x,y,z,t)=-\big(\big(8\sqrt{-\mu_2^2}k\Upsilon+2a_0\mu_2\big)\big(\cos^2(\Upsilon\xi)\big)-4\sqrt{-\mu_2^2}k\Upsilon-2a_0\mu_2\\-2\sin(\Upsilon\xi)\big(-4\Upsilon\mu_2k+\sqrt{-\mu_2^2}a_0\big)\cos(\Upsilon\xi)\big)\\\times\big(2\sin(\Upsilon\xi)\big(\mu_2\sin(\Upsilon\xi)+\sqrt{-\mu_2^2}\cos(\Upsilon\xi)\big)\big)^{-1},\end{aligned}$$

where $\Upsilon=\sqrt{-\mu_2^2/\mu_3}/4$, $\mu_1<0$, $\mu_3>0$, ξ is given in Eqs. (9) and (10);

$$w_6(x,y,z,t)=-\frac{1}{2}k\sqrt{\frac{\mu_2{}^2}{\mu_3}}\tanh\left(\frac{1}{4}\sqrt{\frac{\mu_2{}^2}{\mu_3}}\xi\right)+a_0+\frac{1}{2}k\sqrt{\frac{\mu_2{}^2}{\mu_3}},$$

where $\mu_1>0$, $\Lambda=0$, ξ is given in Eqs. (9) and (10);

$$w_7(x,y,z,t)=-\frac{1}{2}k\sqrt{\frac{\mu_2{}^2}{\mu_3}}\coth\left(\frac{1}{4}\sqrt{\frac{\mu_2{}^2}{\mu_3}}\xi\right)+a_0+\frac{1}{2}k\sqrt{\frac{\mu_2{}^2}{\mu_3}},$$

where $\mu_1>0$, $\Lambda=0$, ξ is given in Eqs. (9) and (10);

$$w_8(x,y,z,t)=-\frac{-\exp\{\frac{1}{2}\sqrt{\frac{\mu_2{}^2}{\mu_3}}\xi\}a_0+\exp\{\frac{1}{2}\sqrt{\frac{\mu_2{}^2}{\mu_3}}\xi\}k\sqrt{\frac{\mu_2{}^2}{\mu_3}}+2a_0\mu_2}{\exp\{\frac{1}{2}\sqrt{\frac{\mu_2{}^2}{\mu_3}}\xi\}-2\mu_2},$$

where $\mu_1>0$, ξ is given in Eqs. (9) and (10);

$$w_9(x,y,z,t)=-\frac{-a_0\xi+2k}{\xi},$$

where $\mu_1=0$, $\mu_2=0$, ξ is given in Eqs. (9) and (10);

- Set 2: $\delta = lk^2\mu_1 + \beta l$, $a_0 = a_0$, $a_1 = \sqrt{\mu_3}k$, $b_1 = 0$, $d_1 = k$, $\mu_1 = \mu_1$.

Therefore, we have the following solutions for Set 2:

$$\begin{aligned} w_{10}(x,y,z,t) = &\left(-\mu_3\left(\mu_1^{3/2}k - a_0\mu_1\right)\left(\tanh^2\left(\frac{\sqrt{\mu_1}\xi}{2}\right)\right)\right. \\ &+ \left(k\sqrt{\mu_1}\mu_2^2 - 2k\mu_1^{3/2}\mu_3 + 2a_0\mu_1\mu_3\right)\tanh\left(\frac{\sqrt{\mu_1}\xi}{2}\right) \\ &\left.+ \sqrt{\mu_3}k\mu_1\mu_2\ \operatorname{sech}\left(\frac{\sqrt{\mu_1}\xi}{2}\right)^2 - k\mu_1^{3/2}\mu_3 + a_0\left(\mu_1\mu_3 - \mu_2^2\right)\right) \\ &\times\left(\mu_1\mu_3\left(1+\tanh\left(\frac{\sqrt{\mu_1}\xi}{2}\right)\right)^2 - \mu_2^2\right)^{-1}, \end{aligned}$$

where $\mu_1 > 0$, ξ is given in Eqs. (9) and (10);

$$\begin{aligned} w_{11}(x,y,z,t) = &\left(-\mu_3\left(\mu_1^{3/2}k - a_0\mu_1\right)\left(\coth^2\left(\frac{\sqrt{\mu_1}\xi}{2}\right)\right)\right. \\ &+ \left(k\sqrt{\mu_1}\mu_2^2 - 2k\mu_1^{3/2}\mu_3 + 2a_0\mu_1\mu_3\right)\coth\left(\frac{\sqrt{\mu_1}\xi}{2}\right) \\ &\left.- \sqrt{\mu_3}\,k\mu_1\mu_2\ \operatorname{csch}\left(\frac{\sqrt{\mu_1}\xi}{2}\right)^2 - k\mu_1^{3/2}\mu_3 + a_0\left(\mu_1\mu_3 - \mu_2^2\right)\right) \\ &\times\left(\mu_1\mu_3\left(1+\coth\left(\frac{\sqrt{\mu_1}\xi}{2}\right)\right)^2 - \mu_2^2\right)^{-1}, \end{aligned}$$

where $\mu_1 > 0$, ξ is given in Eqs. (9) and (10);

$$w_{12}(x,y,z,t) = \frac{a_0(\sqrt{\Lambda}\cosh(\sqrt{\mu_1}\xi) - \mu_2) + 2\sqrt{\mu_3}k\mu_1 - k\sqrt{\mu_1}\sinh(\sqrt{\mu_1}\xi)\sqrt{\Lambda}}{\sqrt{\Lambda}\cosh(\sqrt{\mu_1}\xi) - \mu_2},$$

where $\mu_1 > 0$, $\Lambda > 0$, ξ is given in Eqs. (9) and (10);

$$\begin{aligned} &w_{13}(x,y,z,t) \\ &\quad= \frac{a_0\sqrt{\Lambda}\cos(\sqrt{-\mu_1}\xi) - a_0\mu_2 + 2\sqrt{\mu_3}k\mu_1 + k\sin(\sqrt{-\mu_1}\xi)\sqrt{-\mu_1}\sqrt{\Lambda}}{\sqrt{\Lambda}\cos(\sqrt{-\mu_1}\xi) - \mu_2}, \end{aligned}$$

where $\mu_1 < 0$, $\Lambda > 0$, ξ is given in Eqs. (9) and (10);

$$w_{14}(x,y,z,t) = \frac{(-2k\mu_1\sqrt{\mu_3} + a_0\mu_2)\cosh(\Upsilon) - \sinh(\Upsilon)\sqrt{\mu_1}(k\mu_2 - 2a_0\sqrt{\mu_3})}{2\sqrt{\mu_3}\sqrt{\mu_1}\sinh(\Upsilon) + \mu_2\cosh(\Upsilon)},$$

where $\Upsilon = \sqrt{\mu_1}\,\xi/2$, $\mu_1 > 0$, $\mu_3 > 0$, ξ is given in Eqs. (9) and (10);

$$w_{15}(x,y,z,t) = \left(\left(-2k\sqrt{\mu_3}\mu_1 \tan\left(\frac{\sqrt{-\mu_1}\xi}{2}\right) + \sqrt{-\mu_1}(k\mu_2 + 2a_0\sqrt{\mu_3})\right) \times \sin\left(\frac{\sqrt{-\mu_1}\xi}{2}\right) + a_0\mu_2 \cos\left(\frac{\sqrt{-\mu_1}\xi}{2}\right)\right) \times \left(2\sqrt{\mu_3}\sqrt{-\mu_1}\sin\left(\frac{\sqrt{-\mu_1}\xi}{2}\right) + \mu_2\cos\left(\frac{\sqrt{-\mu_1}\xi}{2}\right)\right)^{-1},$$

where $\mu_1 < 0$, $\Lambda > 0$, ξ is given in Eqs. (9) and (10);

$$w_{16}(x,y,z,t) = \frac{(-2k\mu_1\sqrt{\mu_3} + a_0\mu_2)\sinh(\Upsilon) - \sqrt{\mu_1}(k\mu_2 - 2a_0\sqrt{\mu_3})\cosh(\Upsilon)}{\mu_2\sinh(\Upsilon) + 2\sqrt{\mu_3}\sqrt{\mu_1}\cosh(\Upsilon)},$$

where $\Upsilon = \sqrt{\mu_1}\xi/2$, $\mu_1 > 0$, $\mu_3 > 0$, ξ is given in Eqs. (9) and (10);

$$w_{17}(x,y,z,t) = \frac{k(-2\mu_1\sqrt{\mu_3} - \mu_2\sqrt{\mu_1})\tanh(\frac{\sqrt{\mu_1}\xi}{2}) - 2k\sqrt{\mu_3}\,\mu_1 + (k\sqrt{\mu_1} + 2a_0)\mu_2}{2\mu_2},$$

where $\mu_1 > 0$, $\Lambda = 0$, ξ is given in Eqs. (9) and (10);

$$w_{18}(x,y,z,t) = \frac{k(-2\mu_1\sqrt{\mu_3} - \mu_2\sqrt{\mu_1})\coth(\frac{\sqrt{\mu_1}\xi}{2}) - 2k\sqrt{\mu_3}\,\mu_1 + (k\sqrt{\mu_1} + 2a_0)\mu_2}{2\mu_2},$$

where $\mu_1 > 0$, $\Lambda = 0$, ξ is given in Eqs. (9) and (10);

$$w_{19}(x,y,z,t) = \left((\sqrt{\mu_1}k - a_0)\exp\{2\sqrt{\mu_1}\xi\} + (-4k\sqrt{\mu_3}\mu_1 + 2a_0\mu_2)\exp\{\sqrt{\mu_1}\xi\} - k\sqrt{\mu_1}\mu_2^2 + 4k\mu_1^{3/2}\mu_3 + 4a_0\mu_1\mu_3 - a_0\mu_2^2\right) \times \left(-\exp\{2\sqrt{\mu_1}\xi\} + 2\exp\{\sqrt{\mu_1}\xi\}\mu_2 + 4\mu_1\mu_3 - \mu_2^2\right)^{-1},$$

where $\mu_1 > 0$, ξ is given in Eqs. (9) and (10).

5.2 The F-expansion method

In this section, the amplitude of the traveling wave is analytically solved using the F-expansion method. After balancing v'' with v^2, we get $s = 2$ in Eq. (12). Substituting $s = 2$ into Eq. (17) gives us the following result:

$$v(\xi) = a_0 + a_1F(\xi) + a_2F^2(\xi). \tag{23}$$

By substituting Eq. (23) with Eqs. (18) and (19) into Eq. (12), we obtain the following solution set:

- Set 1:

$$a_0 = 2\left(\frac{Q}{3} + \frac{\sqrt{-3PR + Q^2}}{3}\right)k, \quad a_1 = 0, \quad a_2 = 2Pk, \qquad \delta = 4Qk^2l - 12\left(\frac{Q}{3} + \frac{\sqrt{-3PR + Q^2}}{3}\right)k^2l + \beta l. \tag{24}$$

Plugging Eq. (24) with Eq. (20) into Eq. (23) causes to following cases. In all of the following cases, ξ is given in Eqs. (9) and (10), and c_1 is an arbitrary constant.

Case 1. Choosing (20_1), in the limited case when $m \to 1$, we obtain the soliton-like solution

$$w_{20}(x,y,z,t) = k\left(-2\tanh(\xi) - \ln\big(\tanh(\xi)-1\big) + \ln\big(\tanh(\xi)+1\big) - \frac{2\xi}{3}\right) + c_1. \quad (25)$$

Case 2. Choosing (20_2), in the limited case when $m \to 1$, we obtain the soliton-like solution

$$w_{21}(x,y,z,t) = -\frac{6k\sinh(\xi) - 4k(\xi)\cosh(\xi) - 3c_1\cosh(\xi)}{3\cosh(\xi)}.$$

Case 3. Choosing (20_3), we obtain the following soliton-like solutions: in the limited case when $m \to 1$,

$$w_{22,1}(x,y,z,t) = k\left(-2\coth(\xi) - \ln\big(\coth(\xi)-1\big) + \ln\big(\coth(\xi)+1\big) - \frac{2\xi}{3}\right) + c_1;$$

in the limited case when $m \to 0$,

$$w_{22,2}(x,y,z,t) = \frac{-2k\cos(\xi) + c_1\sin(\xi)}{\sin(\xi)}. \quad (26)$$

Case 4. Choosing (20_4), we obtain the following soliton-like solutions: in the limited case when $m \to 1$,

$$w_{23,1}(x,y,z,t) = -2k\coth(\xi) + \frac{4k\xi}{3} + c_1; \quad (27)$$

in the limited case when $m \to 0$,

$$w_{23,2}(x,y,z,t) = -\frac{2k}{\tan(\xi)} + c_1.$$

Case 5. Choosing (20_5) with $F(\xi,m) = \mathrm{ns}(\xi,m) + \mathrm{cs}(\xi,m)$, we obtain the following soliton-like solutions: in the limited case when $m \to 1$,

$$w_{24,1}(x,y,z,t) = \frac{k(-\ln(\tanh(\frac{\xi}{2})-1) + \ln(\tanh(\frac{\xi}{2})+1) - \frac{2}{\tanh(\frac{\xi}{2})} - \frac{\xi}{3})}{2} + c_1;$$

in the limited case when $m \to 0$,

$$w_{24,2}(x,y,z,t) = -\frac{k}{\tan(\frac{\xi}{2})} + c_1.$$

Case 6. Choosing (20_5) with $F(\xi,m)=\operatorname{ns}(\xi,m)-\operatorname{cs}(\xi,m)$, we obtain the following soliton-like solutions: in the limited case when $m\to 1$, solutions

$$w_{25,1}(x,y,z,t)=\frac{k(-2\tanh(\frac{\xi}{2})-\ln(\tanh(\frac{\xi}{2})-1)+\ln(\tanh(\frac{\xi}{2})+1)-\frac{\xi}{3})}{2}+c_1;$$

in the limited case when $m\to 0$,

$$w_{25,2}(x,y,z,t)=k\tan\left(\frac{\xi}{2}\right)+c_1.$$

Case 7. Choosing (20_6) with $F(\xi,m)=\operatorname{sn}(\xi,m)/(1+\operatorname{cn}(\xi,m))$, we obtain the following soliton-like solutions: in the limited case when $m\to 1$,

$$w_{26,1}(x,y,z,t)=-\frac{k(-3\tanh(\frac{\xi}{2})-\ln(\tanh(\frac{\xi}{2})-1)+\ln(\tanh(\frac{\xi}{2})+1))}{3}+c_1;$$

in the limited case when $m\to 0$,

$$w_{26,2}(x,y,z,t)=k\tan\left(\frac{\xi}{2}\right)+c_1.$$

Case 8. Choosing (20_6) with $F(\xi,m)=\operatorname{sn}(\xi,m)/(1-\operatorname{cn}(\xi,m))$, we obtain the following soliton-like solutions: in the limited case when $m\to 1$,

$$w_{27,1}(x,y,z,t)=\frac{k(\ln(\tanh(\frac{\xi}{2})+1)-\frac{3}{\tanh(\frac{\xi}{2})}-\ln(\tanh(\frac{\xi}{2})-1))}{3}+c_1;$$

in the limited case when $m\to 0$,

$$w_{27,2}(x,y,z,t)=-\frac{k}{\tan(\frac{\xi}{2})}+c_1.$$

Case 9. Choosing (20_7), we obtain the following soliton-like solutions: in the limited case when $m\to 1$,

$$w_{28,1}(x,y,z,t)=\frac{4k(-3\tanh(2\xi)-\ln(\tanh(2\xi)-1)+\ln(\tanh(2\xi)+1))}{3}+c_1;$$

in the limited case when $m\to 0$,

$$w_{28,2}(x,y,z,t)=c_1.$$

Case 10. Choosing (20_8) with $F(\xi,m)=\operatorname{sn}(\xi,m)/(1-\operatorname{cn}(\xi,m))$, we obtain the following soliton-like solutions: in the limited case when $m\to 1$,

$$w_{29,1}(x,y,z,t)=\frac{4k\xi}{3}+c_1;$$

in the limited case when $m \to 0$,

$$w_{29,2}(x,y,z,t) = 2k\tan(\xi) + c_1.$$

Case 11. Choosing (20_9), we obtain the following soliton-like solutions: in the limited case when $m \to 1$,

$$w_{30,1}(x,y,z,t) = \frac{4k\xi}{3} + c_1;$$

in the limited case when $m \to 0$,

$$w_{30,2}(x,y,z,t) = 2k\tan(\xi) - 2k\arctan(\tan(\xi)) + 2k(\xi) + c_1.$$

Case 12. Choosing (20_{10}) with $F(\xi,m) = nc(\xi,m) + \mathrm{sc}(\xi,m)$, we obtain the following soliton-like solutions: in the limited case when $m \to 1$,

$$w_{31,1}(x,y,z,t) = \frac{4k\xi}{3} + c_1;$$

in the limited case when $m \to 0$,

$$w_{31,2}(x,y,z,t) = k\tan(\xi) + c_1 + k\sec(\xi).$$

Case 13. Choosing (20_{10}) with $F(\xi,m) = nc(\xi,m) - \mathrm{sc}(\xi,m)$, we obtain the following soliton-like solutions: in the limited case when $m \to 1$,

$$w_{32,1}(x,y,z,t) = \frac{4k\xi}{3} + c_1;$$

in the limited case when $m \to 0$,

$$w_{32,2}(x,y,z,t) = k\tan(\xi) + c_1 + k\sec(\xi).$$

Case 14. Choosing (20_{11}) with $F(\xi,m) = \mathrm{cn}(\xi,m)/(1+\mathrm{sn}(\xi,m))$, we obtain the following soliton-like solutions: in the limited case when $m \to 1$,

$$w_{33,1}(x,y,z,t) = \frac{4k\xi}{3} + c_1;$$

in the limited case when $m \to 0$,

$$w_{33,2}(x,y,z,t) = -\frac{2k}{\tan(\frac{\xi}{2}) + 1} + c_1.$$

Case 15. Choosing (20_{11}) with $F(\xi,m) = \mathrm{cn}(\xi,m)/(1-\mathrm{sn}(\xi,m))$, we obtain the following soliton-like solutions: in the limited case when $m \to 1$,

$$w_{34,1}(x,y,z,t) = \frac{4k\xi}{3} + c_1;$$

in the limited case when $m \to 0$,

$$w_{34,2}(x,y,z,t) = -\frac{2k}{\tan(\frac{\xi}{2}) - 1} + c_1.$$

Case 16. Choosing (20_{12}), we obtain the following soliton-like solutions: in the limited case when $m \to 1$,

$$\begin{aligned} &w_{35,1}(x,y,z,t) \\ &= \left(-\left(\sqrt{\frac{B^2}{B^2+C^2}}\left(B^2+C^2\right) - B^2\right)(6Bk + \Upsilon C) - \Upsilon C^2 B \tanh\left(\frac{\xi}{2}\right)\right) \\ &\quad \times \left(3\left(\sqrt{\frac{B^2}{B^2+C^2}}\left(B^2+C^2\right) + \tanh\left(\frac{\xi}{2}\right)CB - B^2\right)C\right)^{-1}, \end{aligned}$$

where $\Upsilon = (\ln(\tanh(\xi/2) - 1) - \ln(\tanh(\xi/2) + 1))k - 3c_1$; and in the limited case when $m \to 0$,

$$w_{35,2}(x,y,z,t) = \frac{-C^2 \tan(\frac{\xi}{2})c_1 - 2(Bk - \frac{c_1 C}{2})(\sqrt{\frac{B^2-C^2}{B^2}} - 1)B}{(-\tan(\frac{\xi}{2})C + (\sqrt{\frac{B^2-C^2}{B^2}} - 1)B)C},$$

where ξ is given in Eqs. (9) and (10) and B, C, c_1 is an arbitrary constant.

Case 17. Choosing (20_{13}), we obtain the soliton-like solutions: in the limited case when $m \to 1$, this solution coincides with the one $(w_{35,1})$ obtained in Case 16, in the limited case when $m \to 0$,

$$w_{36,2}(x,y,z,t) = -\frac{2(B^2+C^2)k}{B(B\tan(\xi) + C)} + c_1,$$

where ξ is given in Eqs. (9) and (10) and B, C, c_1 is an arbitrary constant.

6 Results and discussion

In this study, fractional extended shallow-water wave equations with β and M-truncated derivative operators are considered. Despite the different wave transformations, both cases yield the same ODE. All computations and graphical illustrations were carried out and verified using Maple 2023. In this section, $w_1(x,y,z,t)$, $w_2(x,y,z,t)$, $w_{22,2}(x,y,z,t)$, and $w_{23,1}(x,y,z,t)$ solutions in different derivative definitions are considered. Figs. 1–6 provide graphical representations of the fractional operator parameter, allowing for a clear visualization of its effect at different values.

In Fig. 1, we choose $a_0 = 1.2$, $k = 2$, $l = 2$, $\mu_2 = 1$, $\mu_3 = 2$, $n = 1$, $\beta = 1$, $\gamma = 2$. Figure 1(a) visualizes 3D plot for solution $w_1(x,y,z,t)$ with M-truncated derivative, while Fig. 1(b) demonstrates the graph of $w_1(x,y,z,t)$ in the sense of β-derivative with $\alpha = 0.8$. The 3D plot of $w_1(x,y,z,t)$ generated by Eq. (21) depicts a kink pattern. A kink

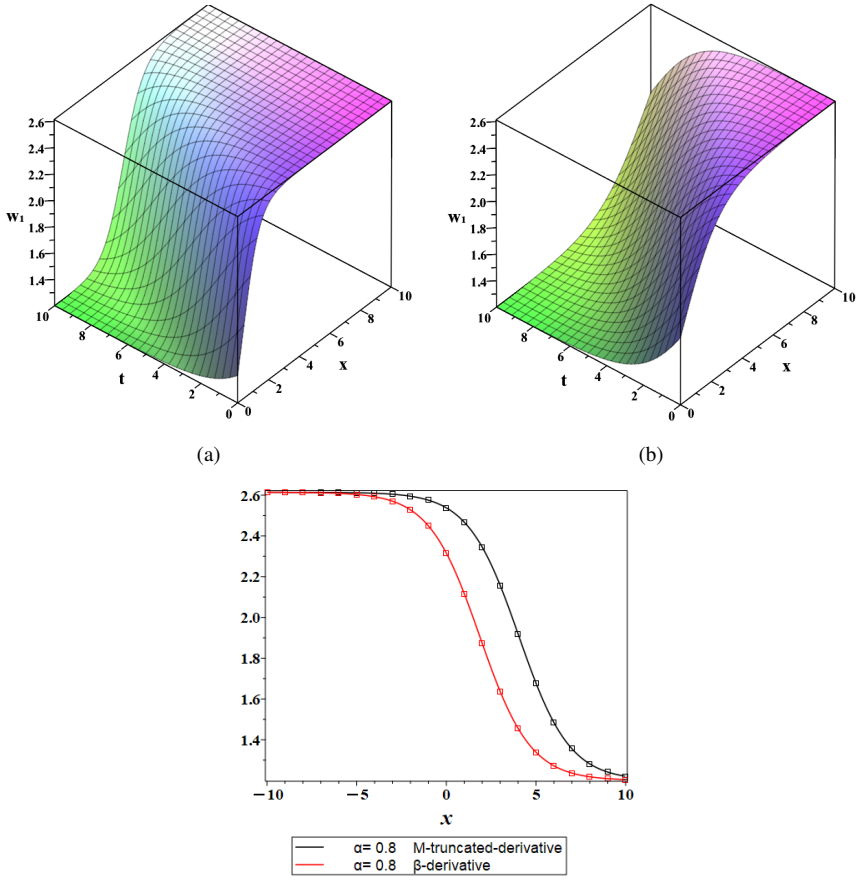

Figure 1. 3D-plot of the solution $w_1(x, y, z, t)$ (21) for M-truncated derivative (a) and β-derivative (b) with $\alpha = 0.8$. (c) depicts the pictorial representation of $w_1(x, y, z, t)$ in 2D-plot using the different definitions of derivatives.

soliton marks the transition of a wave from one asymptotic state to another, illustrating its spatial distribution and propagation at a given time. While both solutions are smooth and soliton-like, the derivative definition mainly alters the steepness and spatial spread, indicating changes in dispersive properties and energy concentration.

Figure 1(c) shows a direct comparison of the kink soliton profiles obtained using the M-truncated and β-derivatives for $\alpha = 0.8$, revealing significant differences in wave behavior. The soliton profile derived from the M-truncated derivative shows a steeper and more localized transition, indicating that energy is more strongly confined and spatial gradients are sharper. On the other hand, the β-derivative generates a wider, more steady shift, indicating increased dispersive effects and a more spread out energy distribution. This comparison demonstrates how the choice of fractional derivative formulation af-

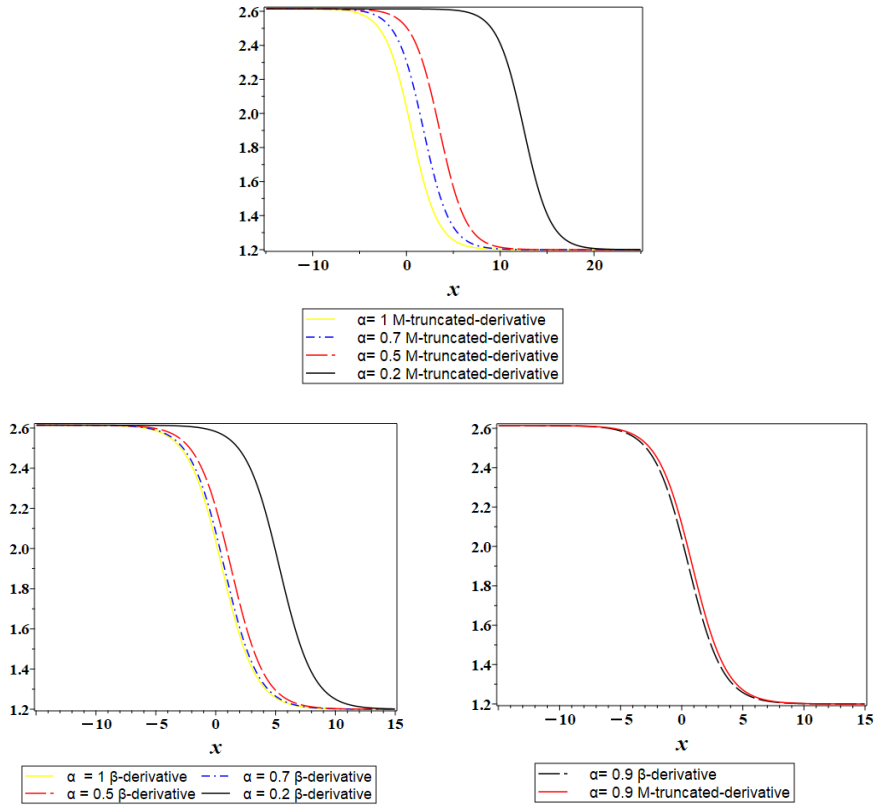

Figure 2. 2D-plots of $w_1(x, y, z, t)$ (21) for different derivatives at $y = z = 1$ and $t = 1$ for different values of α.

fects the structural properties of the soliton. It may also have important implications for modeling physical systems where energy localization or diffusion is critical. The two-dimensional graphs in Fig. 2 show how the wave profile changes as the α value for the M-fractional and β derivatives increase for the same parameters as in Fig. 1. As α decreases from 1 to lower values (e.g., 0.8, 0.5, or 0.2), the slope of the kink becomes progressively smoother, indicating a broader transition region. In the same way, as α decreases from 1 to lower values (e.g., 0.7, 0.5, or 0.2), the slope of the kink becomes smoother. This indicates a broader transition region according to the β-fractional derivative. A decrease in slope flattens the soliton, reducing the field's rate of change and potentially its energy. At $\alpha = 0.9$, both derivative types yield similar soliton profiles, indicating physical consistency. The fractional parameter controls the wave's dispersive and dissipative properties, enabling modeling of systems with memory or hereditary effects.

Figure 3 illustrates the visual depiction of $w_2(x, y, z, t)$ with M-truncated and β derivatives stated in Eq. (22), which is a shock wave solution. This figure is plotted

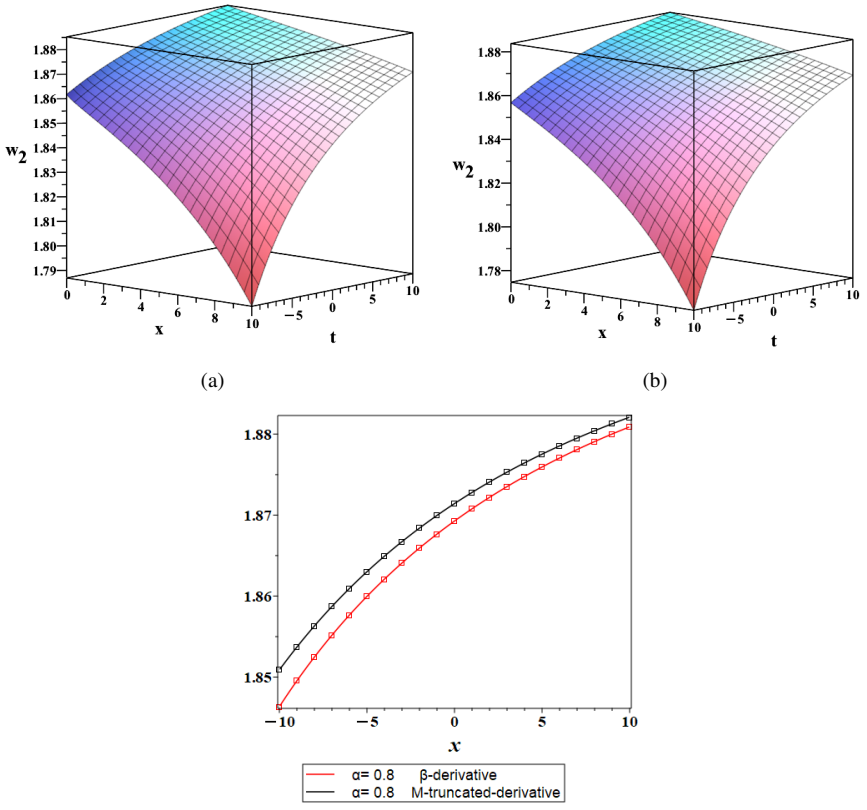

Figure 3. 3D-plot of the solution $w_2(x, y, z, t)$ (22) for $M-$truncated derivative (a) β-derivative (b) with $\alpha = 0.8$. (c) depicts the pictorial representation of $w_2(x, y, z, t)$ in 2D-plot using the different definitions of derivatives.

with $a_0 = 1.9$, $k = .1$, $l = 1$, $\mu_2 = 1$, $\mu_3 = 2$, $n = 1$, $\alpha = .8$, $\beta = 0.2$, $\gamma = 1$. The amplitude and curvature exhibit subtle variations, indicating the mathematical and physical sensitivity to the fractional derivative employed, yet the general wave form is unaltered. Figure 3(c) illustrates 2D-plot for solution $w_2(x, y, z, t)$ with M-truncated and β derivative for same values. Although both curves show a similar upward trend, the M-truncated derivative consistently produces higher values, indicating slightly stronger field variation or energy concentration.

In Fig. 4, we suppose $k = .99$, $l = -0.1$, $n = 0.1$, $\beta = 1$, $\gamma = 1$, $c_1 = 1$. Fig. 4(a) visualizes 3D-plot for $w_{22,2}(x, y, z, t)$ with M-truncated derivative, while Fig. 4(b) images the graph of $w_{22,2}(x, y, z, t)$ in terms of β-derivative with $\alpha = 0.78$. Physically, these features could be singular wave packets or intense concentrated wave energy, which could resemble wave breaking occurrences or rogue wave creation in nonlinear media. In Fig. 5, for the same values as in Fig. 4, the 2D-graphs show how the wave profile changes as the α for the M-fractional and β derivatives increases.

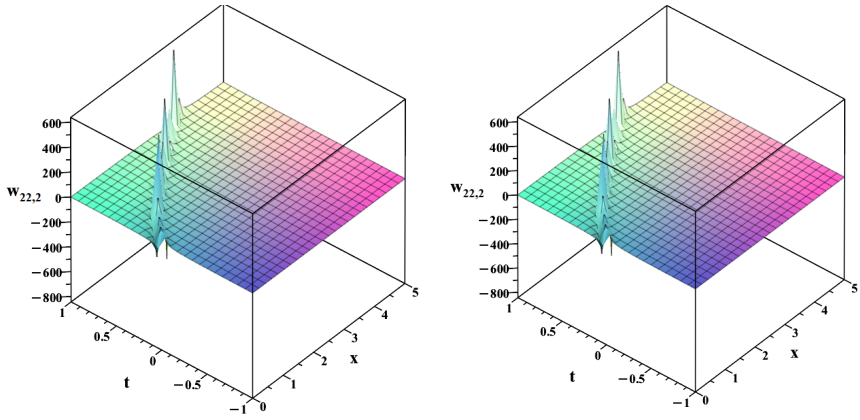

Figure 4. 3D-plot of real part of the solution $w_{22,2}(x,y,z,t)$ (26) for M-truncated derivative (a) and β-derivative (b) with $\alpha = 0.78$.

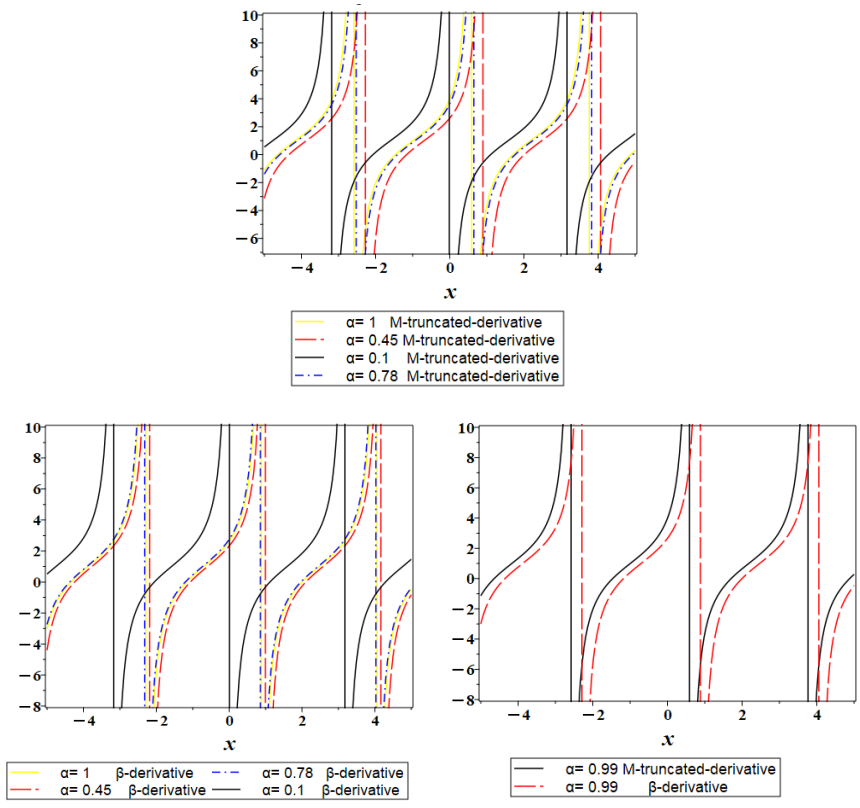

Figure 5. 2D-plots of real part of $w_{22,2}(x,y,z,t)$ (26) for different derivatives at $y = z = 1$ and $t = 2$ for different values of α.

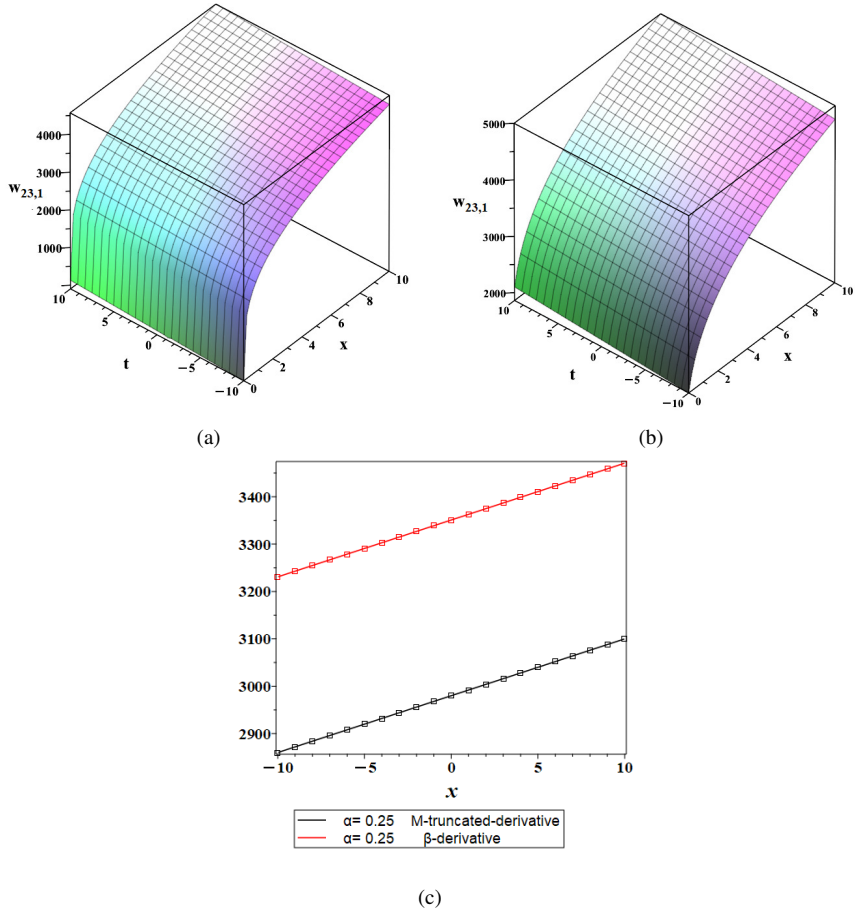

Figure 6. 3D-plot of the solution $w_{23,1}(x, y, z, t)$ (27) for $M-$truncated derivative (a) and β-derivative (b) with $\alpha = 0.25$. (c) depicts the pictorial representation of $w_{23,1}(x, y, z, t)$ (27) in 2D-plot using the different definitions of derivatives.

Figures 6(a) and 6(b) illustrate 3D-plot for solution $w_{23,1}(x, y, z, t)$ with M-truncated and β derivatives with $\alpha = 0.25$, $\beta = 2$, $c_1 = 0$, $\gamma = 0.2$, $k = 3$, $l = 5$, $n = -1$. These figures show that both the M-truncated and β-derivative formulations produce smooth, monotonically increasing solutions when $\alpha = 0.25$. However, a clear difference is observed in the amplitude and growth rate of the solutions: a consistently higher profile is led to by the β-derivative compared to the M-truncated derivative. The 2D-plot in Fig. 6(c) shows a steeper slope for the β-derivative solution, indicating faster variation with respect to x.

For the classical case $\alpha = 1$ and $\beta = 0$, the equation given in (6) was previously investigated in [30] and [29], where multiple singular and multiple-singular soliton solutions were obtained, respectively. Additionally, exact solutions were derived using the (G'/G) method in [7] for $\alpha = 1$. A comparison with these earlier results suggests that the

findings of the present study offer new insights. The present analysis provides a broader range of solutions through the use of two fractional derivative operators, offering deeper insight into solution structures and highlighting the influence of fractional-order dynamics on system behavior.

7 Modulation instability analysis

Modulation instability (MI) analysis [14] for the stationary solutions of Eq. (5) is examined in this section of the study under the assumption that Eq. (5) has the following stationary solution:

$$h(x,y,z,t) = P_0 + v\psi(x,y,z,t), \tag{28}$$

where P_0 stands for a steady flow attitude for Eq. (5), and v is arbitrary constant. We use the principle of linear stability analysis to examine the evolution of the perturbation $\phi(x,y,z,t)$. Substituting Eq. (28) into Eq. (6) and linearizing, we obtain

$$\psi_{txz} + \psi_{xxxyz} + \beta\psi_{xyz} = 0. \tag{29}$$

Suppose solutions of Eq. (29) in the following form:

$$\phi(x,y,z,t) = \mathrm{e}^{\mathrm{i}(ax+by+cz-dt)}, \tag{30}$$

where d is the frequency of perturbation, and a, b, and c are normalized wave numbers. Equations (29) and (30) jointly provide $d+a^2b-\beta b = 0$. Then we can write the following:

$$d = -a^2b + \beta b. \tag{31}$$

The given equation has been subjected to an analysis of stability using the linear stability approach, and the results show that it is stable Fig. 7.

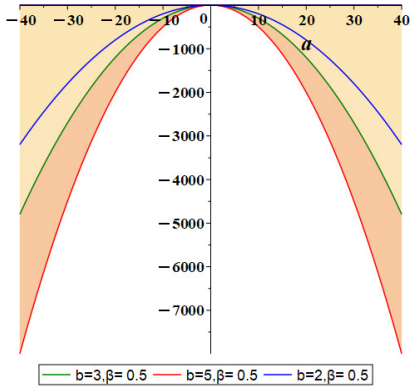

Figure 7. The modulation instability graphs for $b = 2, 3, 5$ and $\beta = 0.5$ in Eq. (31).

8 Conclusion

In this work, we have determined the optical solitons of the fractional extended shallow-water wave equations using β- and M-truncated derivatives. Shallow-water wave equations are helpful for resembling physical systems because of their often strong structure. The details of these solutions are obtained by the F-expansion approach and the extended modified auxiliary equation mapping method. These techniques have been successfully applied to find new solutions used to create a wide variety of solutions for trigonometric, hyperbolic, and rational functions. As can be seen in Figs. 1–6, graphical visualizations clearly demonstrate the influence of the fractional order α and the choice of derivative operator on wave dynamics. Notably, the M-truncated and β-derivative solutions differ significantly in terms of steepness, amplitude modulation, and dispersion characteristics. The linear stability of these solitons was validated using MI analysis (see Fig. 7), which confirms the robustness of the derived wave structures under small perturbations. Building on previous studies, including those using classical derivatives, the present results offer a more comprehensive perspective while remaining consistent with established findings. These findings highlight the flexibility of the employed methodologies, applicable to higher-dimensional models and other fractional PDEs in fluid mechanics, nonlinear optics, plasma physics, and geophysical flows. Comparative analysis of different fractional derivatives further provides insights into modeling accuracy and physical fidelity, enabling improved simulation of complex nonlinear phenomena.

Author contributions. The authors contributed equally to this work. The published version of the manuscript has been read and approved by both authors.

Conflicts of interest. The authors declare no conflicts of interest.

References

1. K. Ali, S. Tarla, M. Ali, A. Yusuf, Modulation instability analysis and optical solutions of an extended $(2+1)$-dimensional perturbed nonlinear Schrödinger equation, *Results Phys.*, **45**: 106255, 2023, https://doi.org/10.1016/j.rinp.2023.106255.
2. K.K. Ali, S. Tarla, M.R. Ali, A. Yusuf, R. Yilmazer, Physical wave propagation and dynamics of the Ivancevic option pricing model, *Results Phys.*, **52**:106751, 2023, https://doi.org/10.1016/j.rinp.2023.106751.
3. K.K. Ali, A. Yusuf, A. Yokus, M.R. Ali, Optical waves solutions for the perturbed Fokas–Lenells equation through two different methods, *Results Phys.*, **53**:106869, 2023, https://doi.org/10.1016/j.rinp.2023.106869.
4. A. Atangana, D. Baleanu, A. Alsaedi, Analysis of time-fractional Hunter-Saxton equation: A model of neumatic liquid crystal, *Open Phys.*, **14**(1):145–149, 2016, https://doi.org/10.1515/phys-2016-0010.
5. D. Baleanu, B. Agheli, M.M. Al Qurashi, Fractional advection differential equation within Caputo and Caputo–Fabrizio derivatives, *Adv. Mech. Eng.*, **8**(12):1687814016683305, 2017, https://doi.org/10.1177/1687814016683305.

6. D. Baleanu, A. Atangana, New fractional derivatives with nonlocal and non-singular kernel: Theory and application to heat transfer model, *Therm. Sci.*, **20**:763–769, 2016, https://doi.org/10.2298/TSCI160111018A.
7. A. Bekir, E. Aksoy, Exact solutions of shallow water wave equations by using the $(\frac{G'}{G})$-expansion method, *Waves Random Complex Media*, **22**(3):317–331, 2012, https://doi.org/10.1080/17455030.2012.683890.
8. L. Cheng, Y. Zhang, W.X. Ma, An extended $(2+1)$-dimensional modified Korteweg–de Vries–Calogero–Bogoyavlenskii–Schiff equation: Lax pair and Darboux transformation, *Commun. Theor. Phys.*, **77**(3):035002, 2025, https://doi.org/10.1088/1572-9494/ad84d3.
9. J.Y. Chu, Y.Q. Liu, W.X. Ma, Integrability and multiple-rogue and multi-soliton wave solutions of the $(3+1)$-dimensional Hirota–Satsuma–Ito equation, *Mod. Phys. Lett. B*, **39**:2550060, 2025, https://doi.org/10.1142/S0217984925500605.
10. P.A. Clarkson, E.L. Mansfield, On a shallow water wave equation, *Nonlinearity*, **7**:975, 1994, https://doi.org/10.1088/0951-7715/7/3/012.
11. A.N. Gerasimov, Generalization of laws of the linear deformation and their application to problems of the internal friction, *Prikl. Mat. Mekh.*, **12**:251–260, 1948 (in Russian).
12. C. Huai-Tang, Z. Hong-Qing, New double periodic and multiple soliton solutions of the generalized $(2+1)$-dimensional Boussinesq equation, *Chaos Solitons Fractals*, **20**(4):765–769, 2004, https://doi.org/10.1016/j.chaos.2003.08.006.
13. A. Hussain, A. Jhangeer, N. Abbas, I. Khan, E.S.M. Sherif, Optical solitons of fractional complex Ginzburg–Landau equation with conformable, beta, and M-truncated derivatives: A comparative study, *Adv. Difference Equ.*, **2020**:612, 2020, https://doi.org/10.1186/s13662-020-03052-7.
14. K. Khan, M.A. Akbar, Study of explicit travelling wave solutions of nonlinear evolution equations, *Partial Differ. Equations Appl. Math.*, **7**:100475, 2023, https://doi.org/10.1016/j.padiff.2022.100475.
15. W.X. Ma, Lump waves and their dynamics of a spatial symmetric generalized KP model, *Rom. Rep. Phys.*, **76**:108–108, 2024, https://doi.org/10.59277/RomRepPhys.2024.76.108.
16. W.X. Ma, Y. Zhou, Lump solutions to nonlinear partial differential equations via Hirota bilinear forms, *J. Differ. Equations*, **264**(4):2633–2659, 2018, https://doi.org/10.1016/j.jde.2017.10.033.
17. J.T. Machado, V. Kiryakova, F. Mainardi, Recent history of fractional calculus, *Commun. Nonlinear Sci. Numerical Simul.*, **16**(3):1140–1153, 2011, https://doi.org/10.1016/j.cnsns.2010.05.027.
18. K. Mukdasai, Z. Sabir, M.A.Z. Raja, R. Sadat, M.R. Ali, P. Singkibud, A numerical simulation of the fractional order Leptospirosis model using the supervise neural network, *Alexandria Eng. J.*, **61**(12):12431–12441, 2022, https://doi.org/10.1016/j.aej.2022.06.013.
19. Y.S. Özkan, The exact solutions of the Shynaray-IIA equation along with analysis of bifurcation and chaotic behaviors, *Qual. Theory Dyn. Syst.*, **23**(Suppl 1):288, 2024, https://doi.org/10.1007/s12346-024-01153-2.

20. M. Sadaf, S. Arshed, G. Akram, M. Ali, I. Bano, Analytical investigation and graphical simulations for the solitary wave behavior of Chaffee-Infante equation, *Results Phys.*, **54**: 107097, 2023, https://doi.org/10.1016/j.rinp.2023.107097.

21. S.G. Samko, A.A. Kilbas, O.I. Marichev, *Fractional Integrals and Derivatives: Theory and Applications*, Gordon and Breach, New York, 1993.

22. A.C. Scott, *Encyclopedia of Nonlinear Science*, Routledge, New York, 2005, https://doi.org/10.4324/9780203647417.

23. A.R. Seadawy, N. Cheemaa, Applications of extended modified auxiliary equation mapping method for high-order dispersive extended nonlinear Schrödinger equation in nonlinear optics, *Mod. Phys. Lett. B*, **33**(18):1950203, 2019, https://doi.org/10.1142/S0217984919502038.

24. A.R. Seadawy, N. Cheemaa, A. Biswas, Optical dromions and domain walls in $(2+1)$-dimensional coupled system, *Optik*, **227**:165669, 2021, https://doi.org/10.1016/j.ijleo.2020.165669.

25. A. Shahzad, F. Liaqat, Z. Ellahi et al., Thin film flow and heat transfer of Cu-nanofluids with slip and convective boundary condition over a stretching sheet, *Sci. Rep.*, **12**:14254, 2022, https://doi.org/10.1038/s41598-022-18049-3.

26. J.V. Sousa, E.C. de Oliveira, A new truncated Mfractional derivative type unifying some fractional derivative types with classical properties, *Int. J. Anal. Appl.*, **16**:83–96, 2018, https://doi.org/10.28924/2291-8639-16-2018-83.

27. M. Umar, F. Amin, Q. Al-Mdallal, M.R. Ali, A stochastic computing procedure to solve the dynamics of prevention in HIV system, *Biomed. Signal Process. Control*, **78**:103888, 2022, https://doi.org/10.1016/j.bspc.2022.103888.

28. A.M. Wazwaz, Multiple soliton solutions and multiple-singular soliton solutions for $(2+1)$-dimensional shallow water wave equations, *Phys. Lett. A*, **373**:2927, 2009, https://doi.org/10.1016/j.physleta.2009.06.026.

29. A.M. Wazwaz, Multiple soliton solutions and multiple-singular soliton solutions for two higher-dimensional shallow water wave equations, *Appl. Math. Comput.*, **211**:495, 2009, https://doi.org/10.1016/j.amc.2009.01.071.

30. A.M. Wazwaz, Multiple-soliton solutions for extended shallow water wave equations, *Stud. Math. Sci.*, **1**(1):21–29, 2010.